

Electronic Supplementary Information

Near-saturated red emitters: four-coordinate copper(I) halide complexes containing 8-(diphenylphosphino)quinoline and 1-(diphenylphosphino)naphthalene ligands

Li-Ping Liu, Qian Li, Song-Po Xiang, Li Liu*, Xin-Xin Zhong, Chen Liang, Guang Hua Li*, Tasawar Hayat, Njud S. Alharbi, Fa-Bao Li*, Nian-Yong Zhu, Wai-Yeung Wong*, Hai-Mei Qin, Lei Wang*

Contents

Experimental Details

1. NMR Experiments

Fig. S1 ^1H NMR spectrum of **1** in CDCl_3 .

Fig. S2 ^1H NMR spectrum of **2** in CDCl_3 .

Fig. S3 ^1H NMR spectrum of **3** in CDCl_3 .

Fig. S4 ^{31}P NMR spectrum of **1** in CDCl_3 .

Fig. S5 ^{31}P NMR spectrum of **2** in CDCl_3 .

Fig. S6 ^{31}P NMR spectrum of **3** in CDCl_3 .

2. Molecular structures

Fig. S7. 1-D molecular structure and C–H \cdots π interactions in **1**.

Fig. S8. 1-D molecular structure and C–H \cdots π interactions in **2**.

Fig. S9. 1-D molecular structure and C–H \cdots π interactions in **3**.

3. Photophysical properties

Fig. S10. Time profiles of luminescence decay and exponential fit spectrum of **1** at r.t.

Fig. S11. Time profiles of luminescence decay and exponential fit spectrum of **2** at r.t.

Fig. S12. Time profiles of luminescence decay and exponential fit spectrum of **3** at r.t

Fig. S13. Emission spectra of dpqu, dpna and complexes **1–3** in degassed CH_2Cl_2 at 293 K with the concentrations of 2.5×10^{-4} M.

Fig. S14. PL spectra of complex **1** in CH₃CN/water mixture with different water fractions (f_w). The inset shows a magnified view of the emission from 400 to 470 nm. The concentrations are 5×10^{-4} M.

4. Computational details

Fig. S15. The absorption spectrum of complex **1** in CH₂Cl₂.

Fig. S16. The absorption spectrum of complex **2** in CH₂Cl₂.

Fig. S17. The absorption spectrum of complex **3** in CH₂Cl₂.

Fig. S18. Contour plots of frontier molecular orbitals of complexes **1-3** in CH₂Cl₂.

Fig. S19. Contour plots of frontier molecular orbitals at the first excited state geometries of complexes **2** and **3**.

Table S1. Energy and compositions of frontiers molecular orbitals of complex **1** in CH₂Cl₂.

Table S2. Energy and compositions of frontiers molecular orbitals of complex **2** in CH₂Cl₂.

Table S3. Energy and compositions of frontiers molecular orbitals of complex **3** in CH₂Cl₂.

Table S4. Computed excitation states for complex **1** in CH₂Cl₂.

Table S5. Computed excitation states for complex **2** in CH₂Cl₂.

Table S6. Computed excitation states for complex **3** in CH₂Cl₂.

Table S7. Calculated emission wavelength (λ), oscillator strength (f) and main configuration of complexes **2-3** along with their experimental values (λ_{exp}).

Experimental Details

1. NMR Experiments

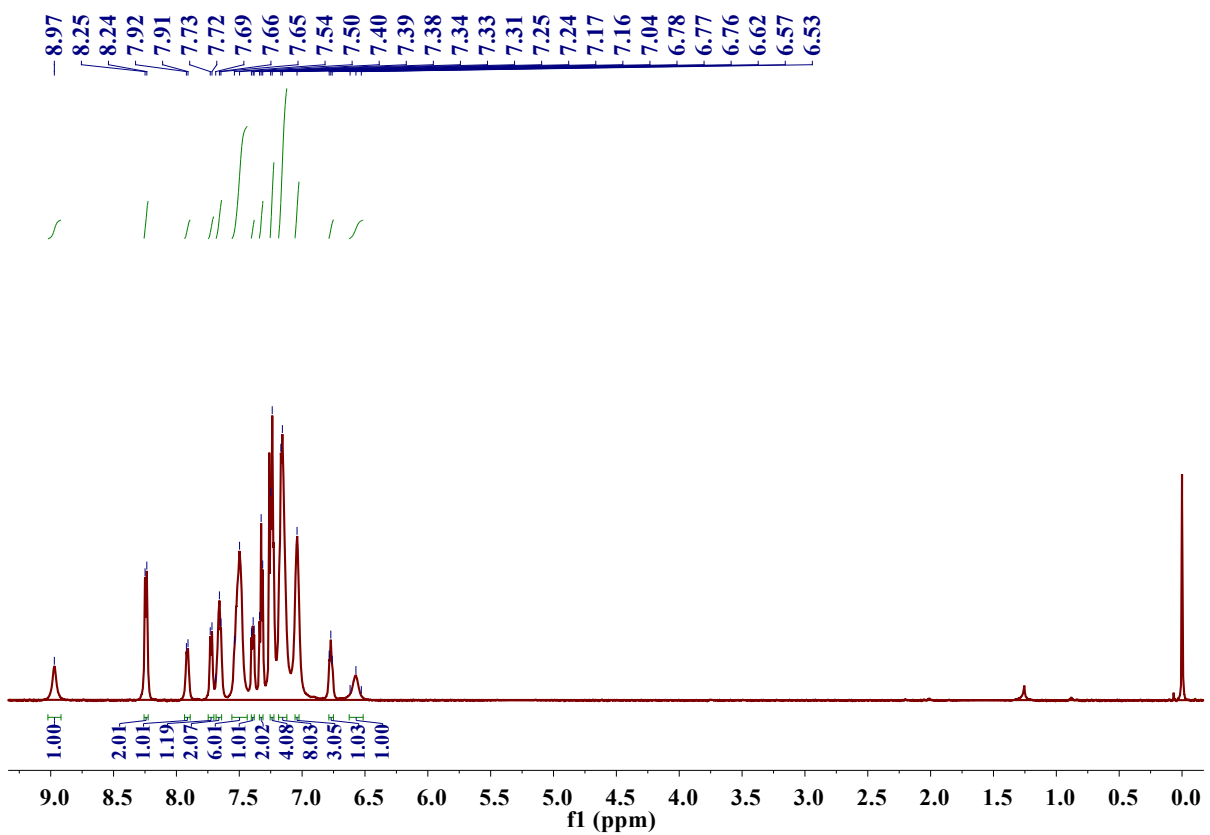


Fig. S1. ^1H NMR spectrum of **1** in CDCl_3 .

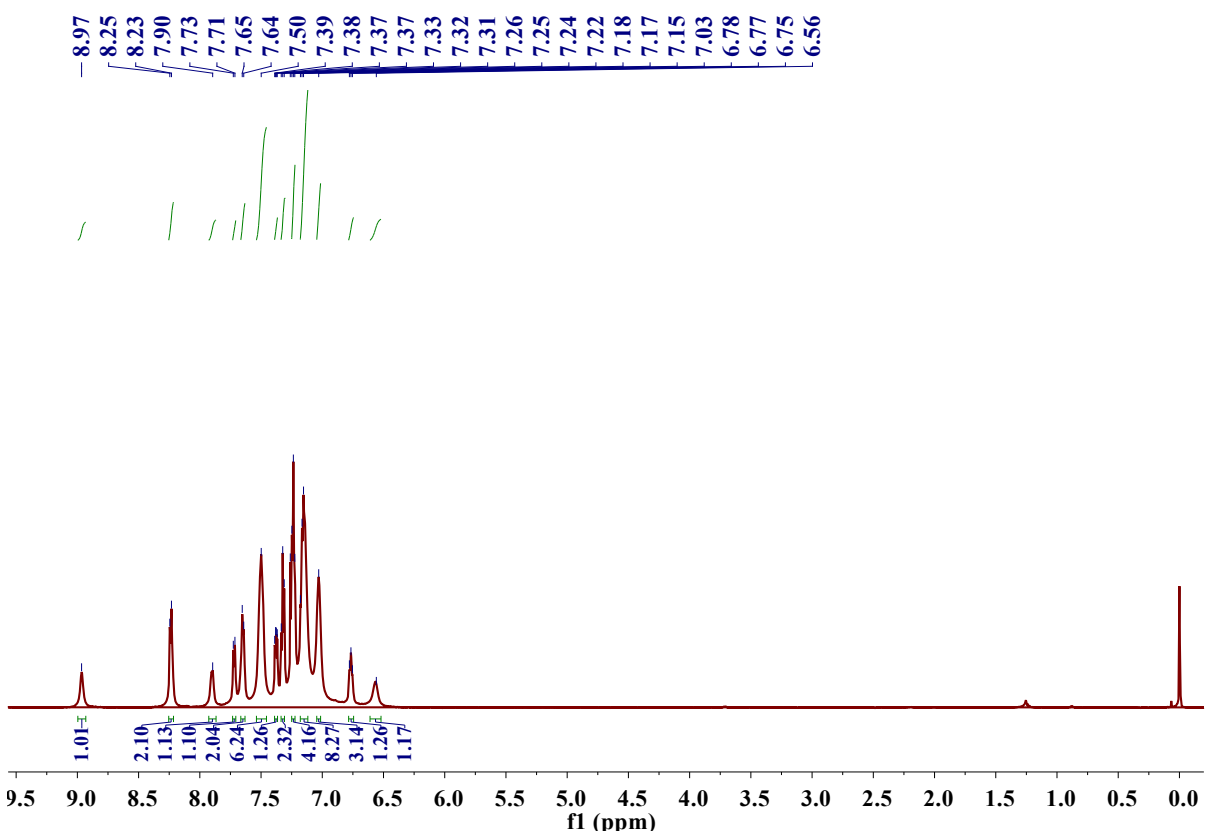


Fig. S2. ^1H NMR spectrum of **2** in CDCl_3 .

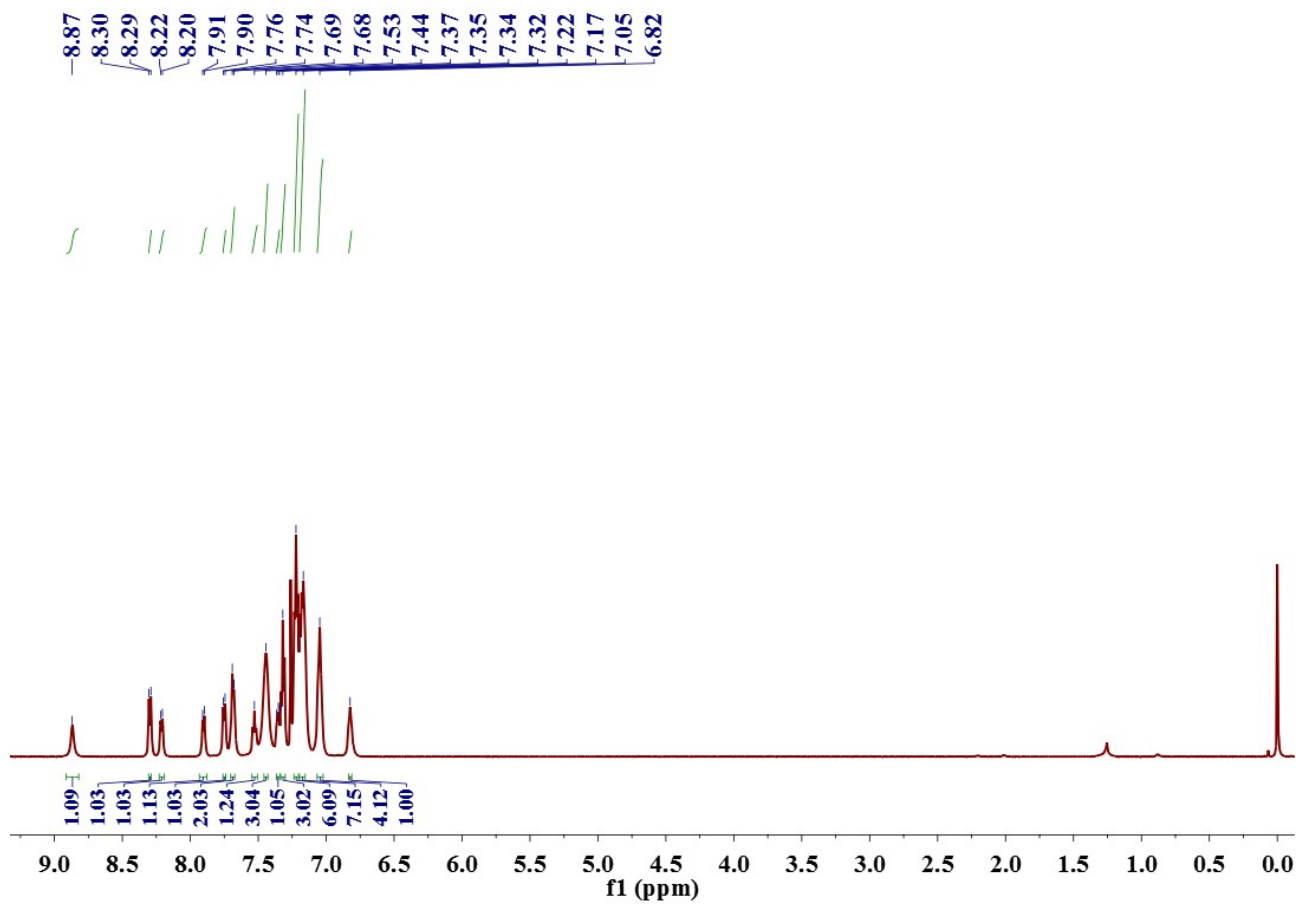


Fig. S3. ^1H NMR spectrum of **3** in CDCl_3 .

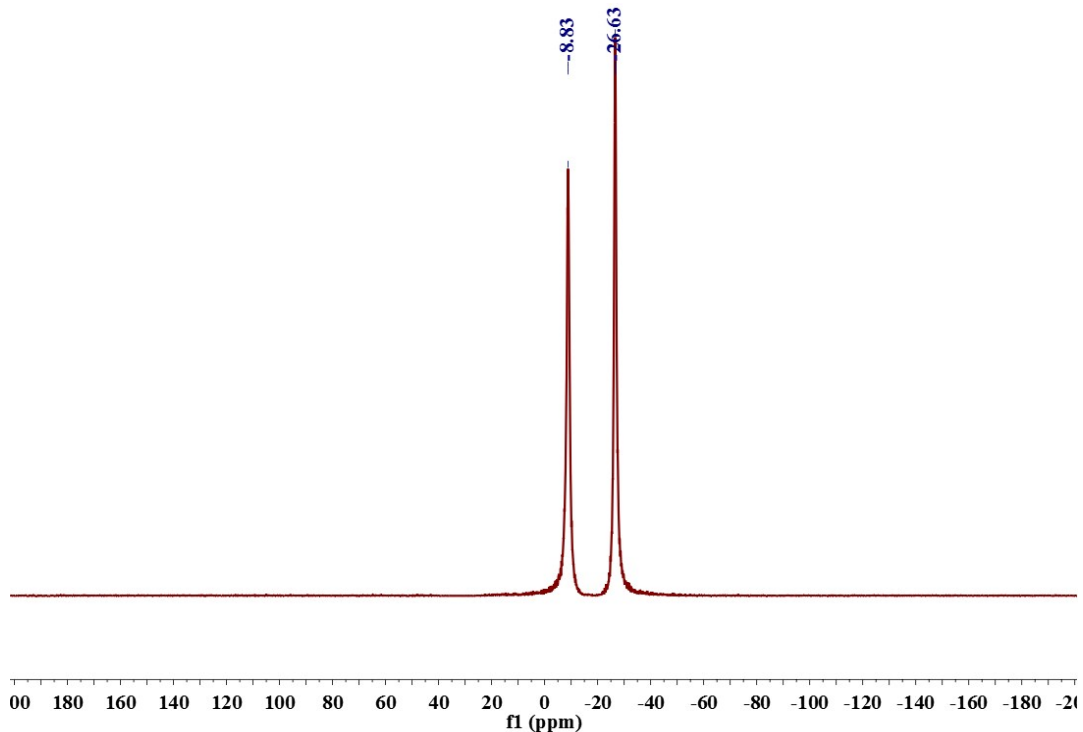


Fig. S4. ^{31}P NMR spectrum of **1** in CDCl_3 .

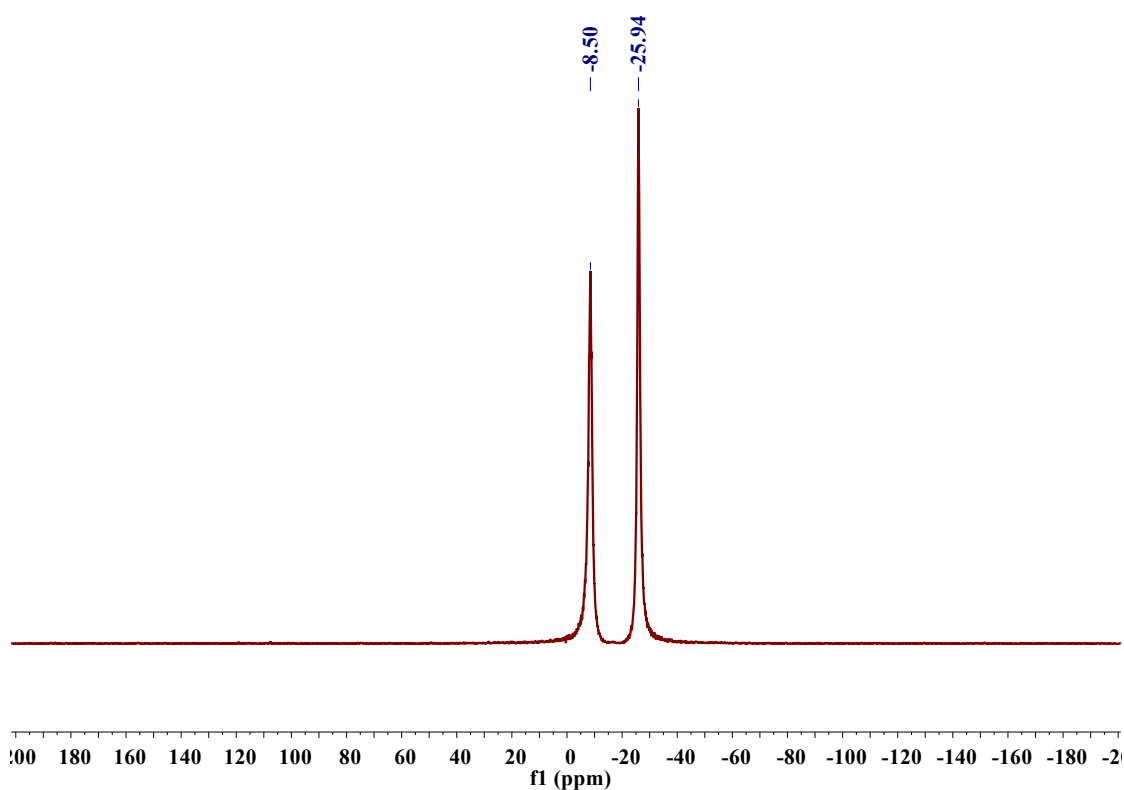


Fig. S5. ^{31}P NMR spectrum of **2** in CDCl_3 .

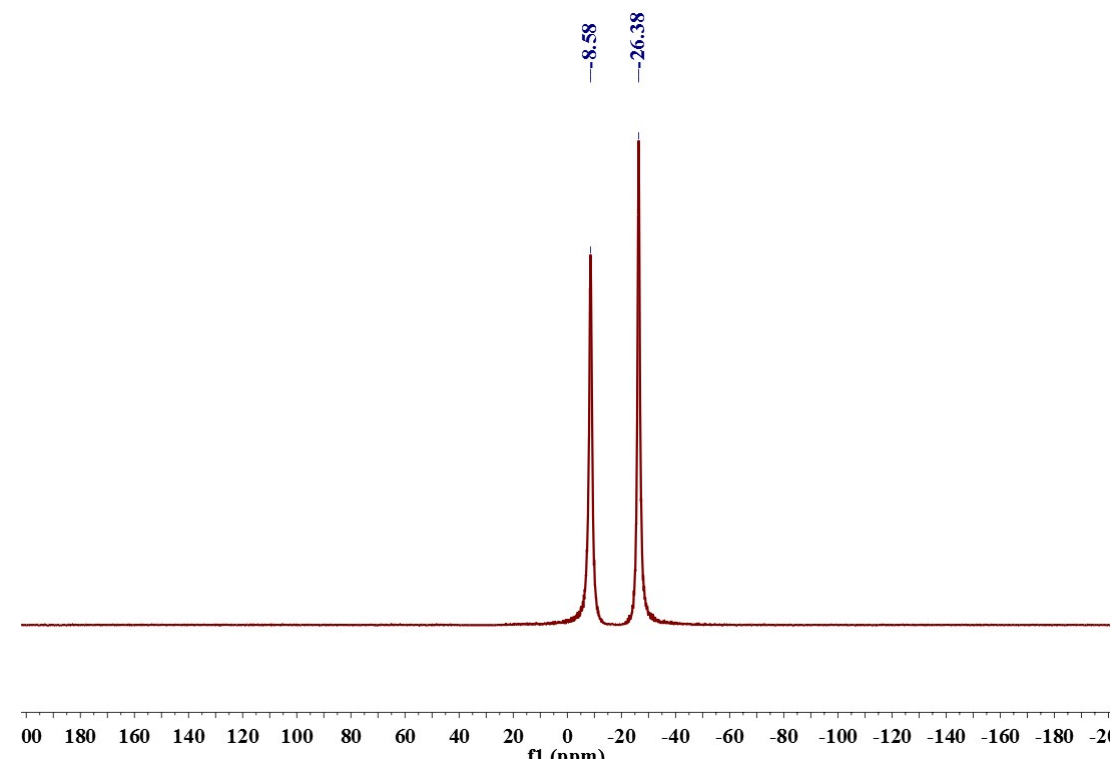


Fig. S6. ^{31}P NMR spectrum of **3** in CDCl_3 .

2. Molecular structures

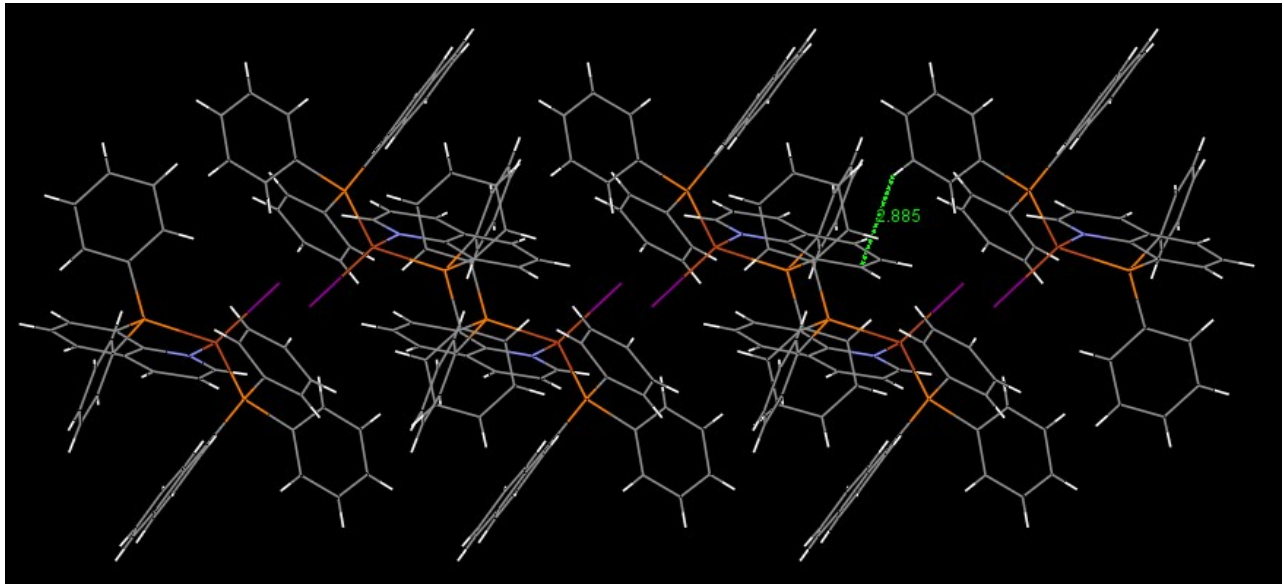


Fig. S7. 1-D molecular structure and C–H \cdots π interactions in **1**.

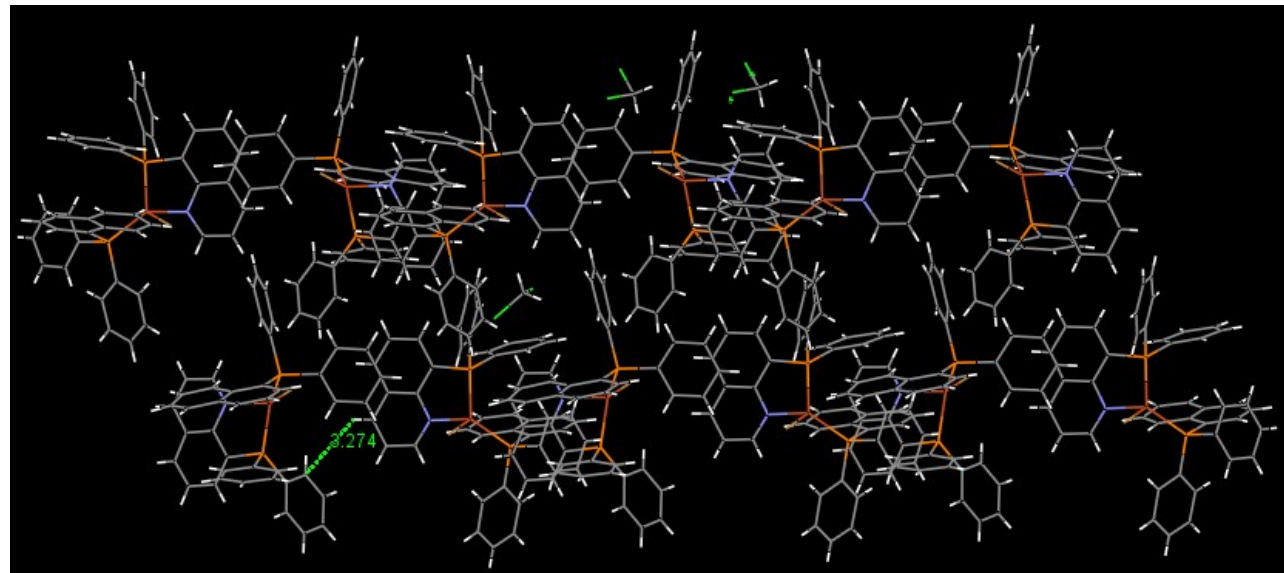


Fig. S8. 1-D molecular structure and C–H \cdots π interactions in **2**.

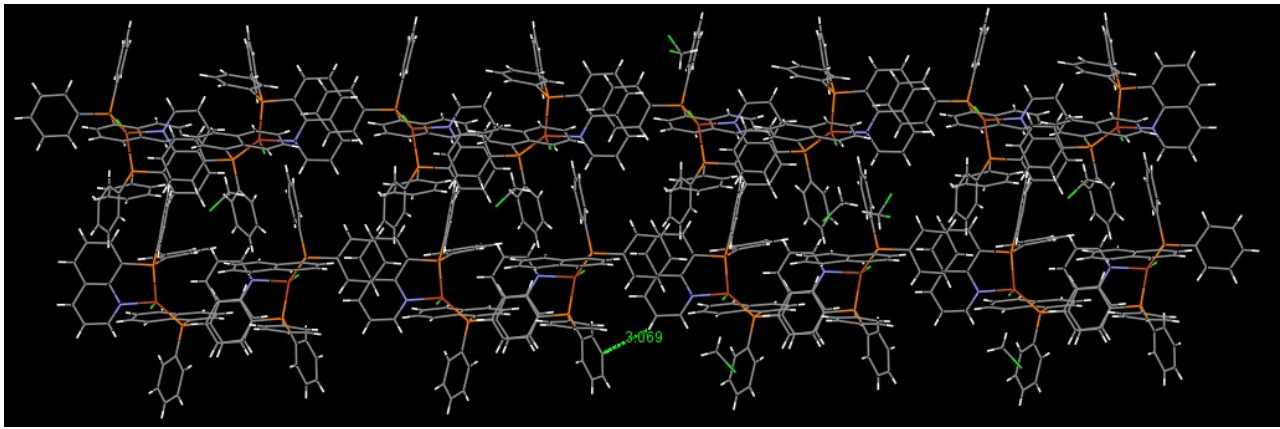


Fig. S9. 1-D molecular structure and C–H \cdots π interactions in **3**.

3. Photophysical properties

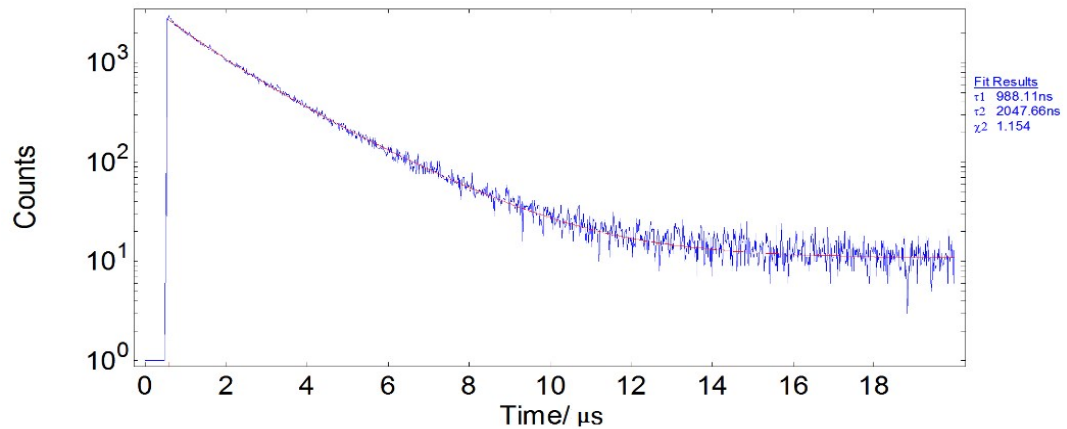


Fig. S10. Time profiles of luminescence decay and exponential fit spectrum of **1** at r.t.

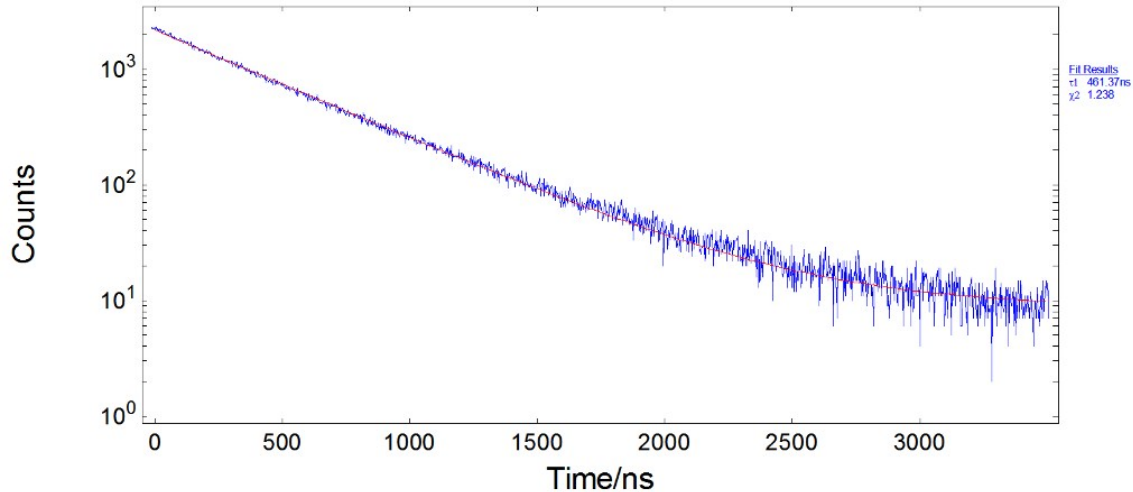


Fig. S11. Time profiles of luminescence decay and exponential fit spectrum of **2** at r.t.

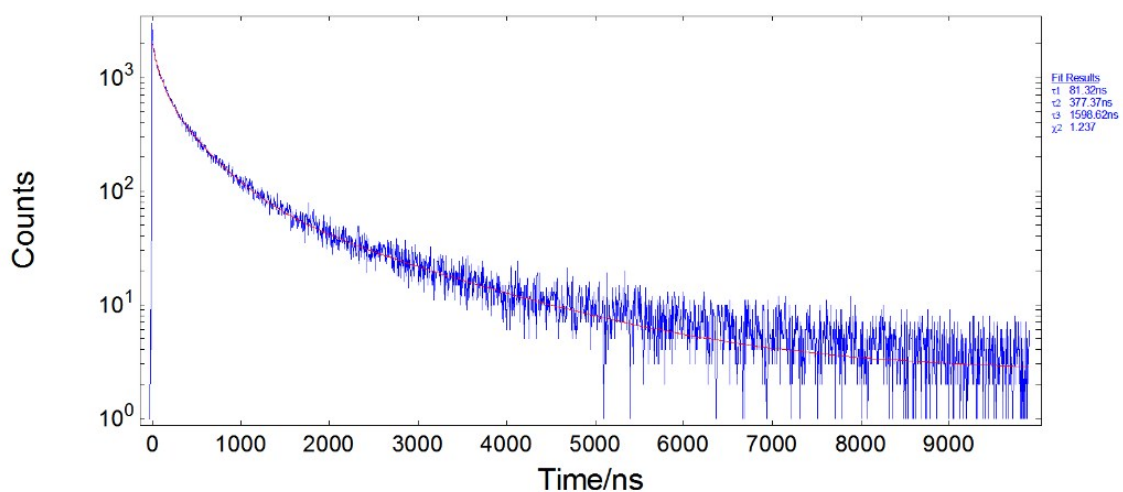


Fig. S12. Time profiles of luminescence decay and exponential fit spectrum of **3** at r.t.

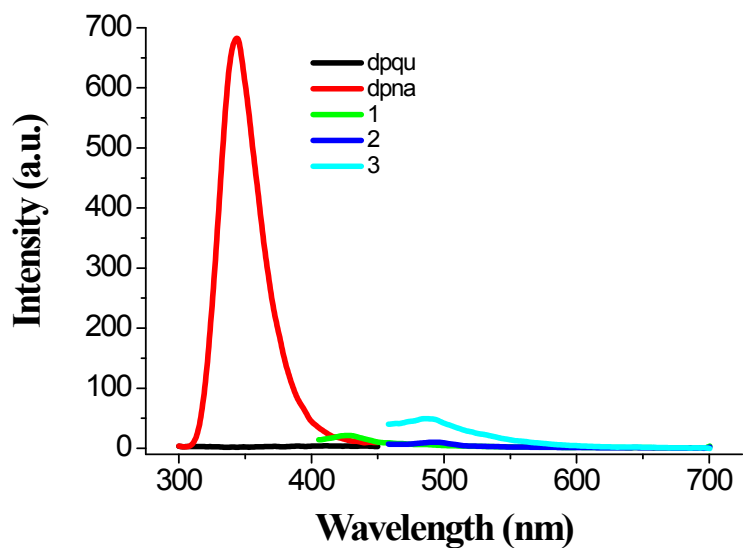


Fig. S13. Emission spectra of dpqu, dpna and complexes **1–3** in degassed CH_2Cl_2 at 293 K with the concentrations of 2.5×10^{-4} M.

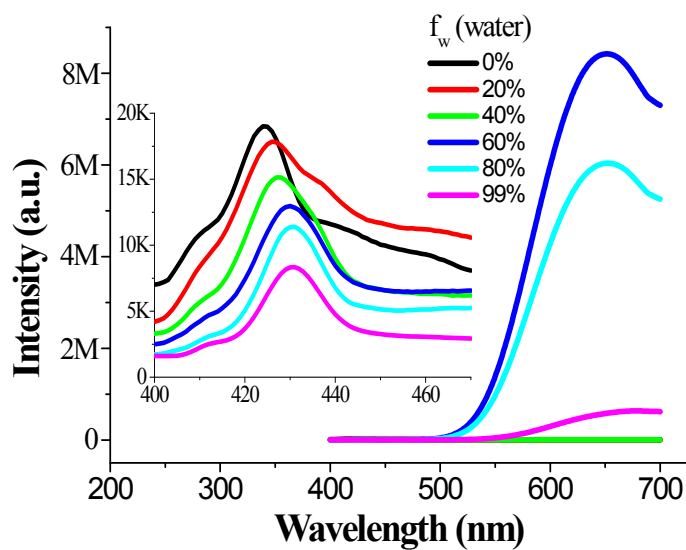


Fig. S14. PL spectra of complex **1** in CH_3CN /water mixture with different water fractions (f_w). The inset shows a magnified view of the emission from 400 to 470 nm. The concentrations are 5×10^{-4} M.

4. Computational details

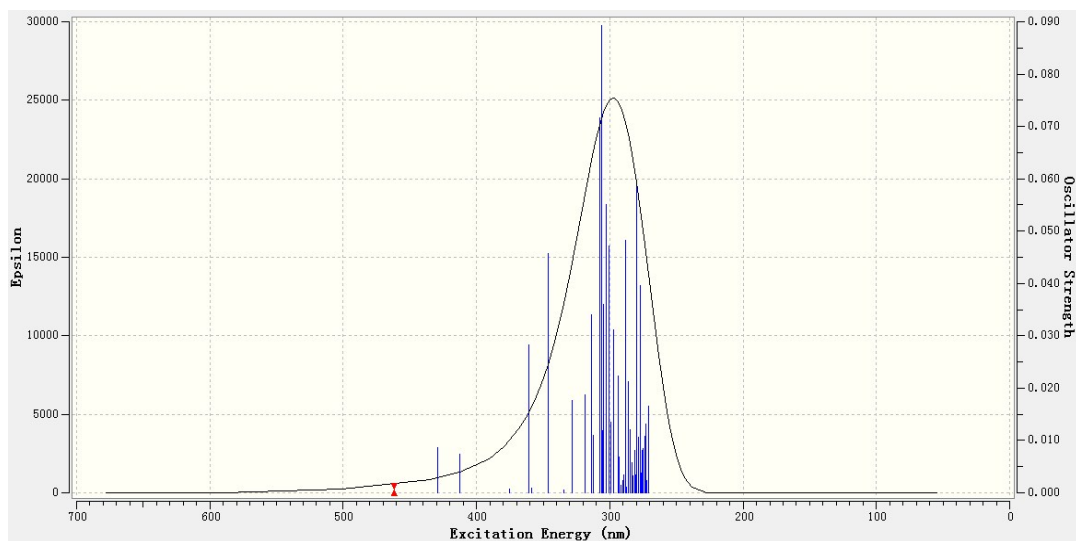


Fig. S15. The absorption spectrum of complex **1** in CH_2Cl_2 .

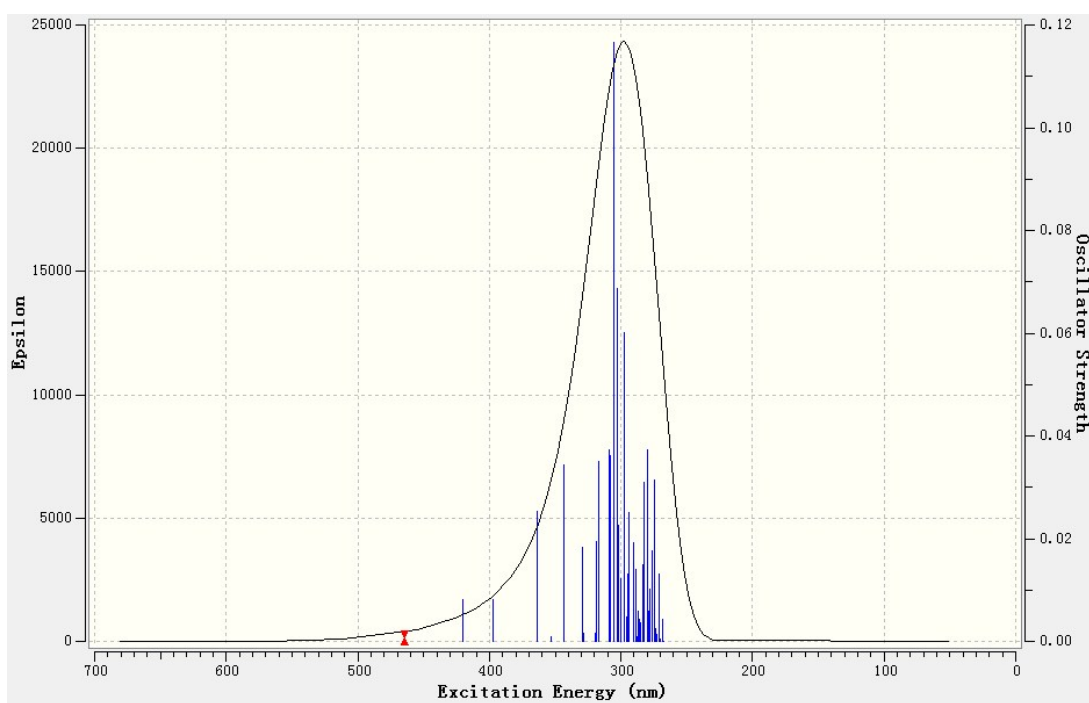


Fig. S16. The absorption spectrum of complex **2** in CH_2Cl_2 .

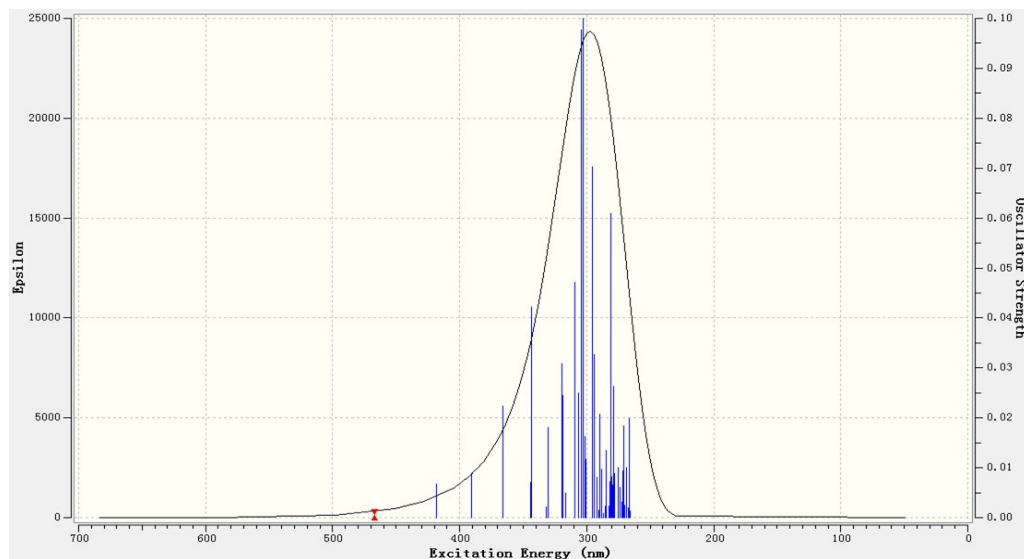
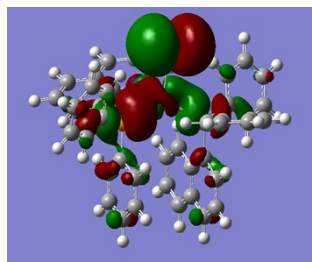
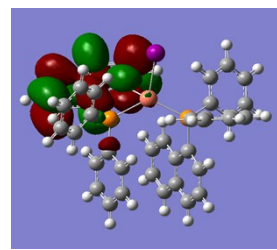


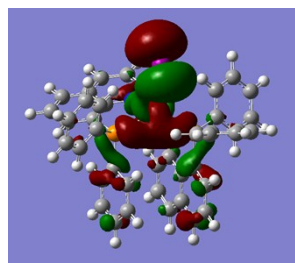
Fig. S17. The absorption spectrum of complex **3** in CH_2Cl_2 .



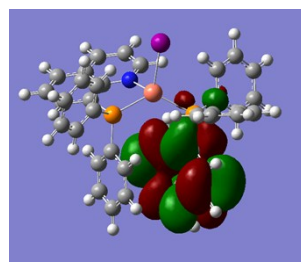
HOMO



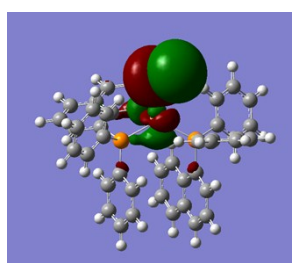
LUMO



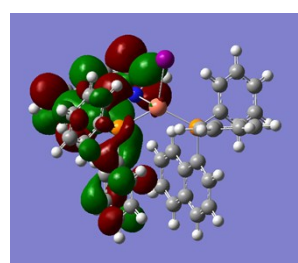
HOMO-1



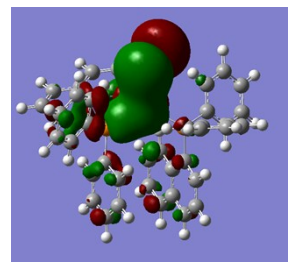
LUMO+1



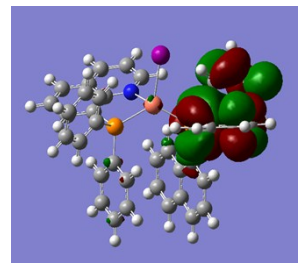
HOMO-2



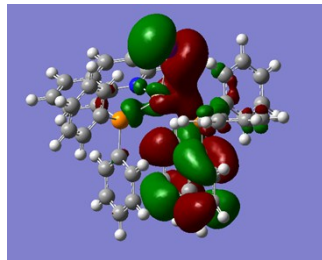
LUMO+2



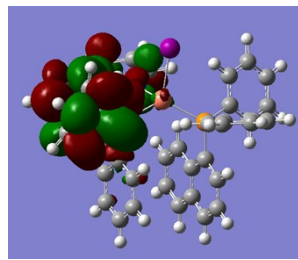
HOMO-3



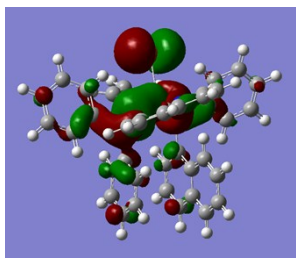
LUMO+3



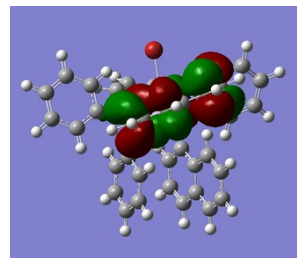
HOMO-4



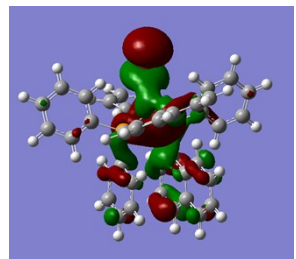
LUMO+4



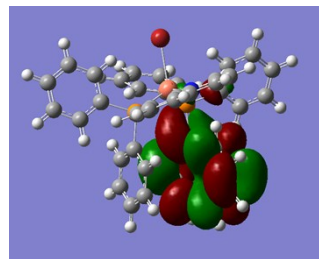
HOMO



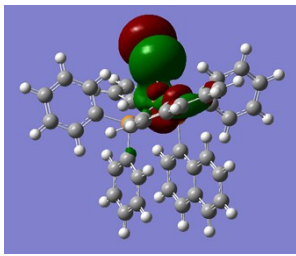
LUMO



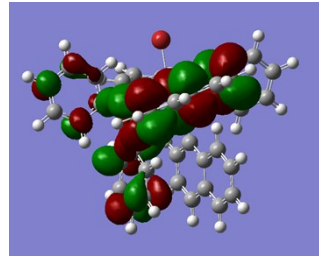
HOMO-1



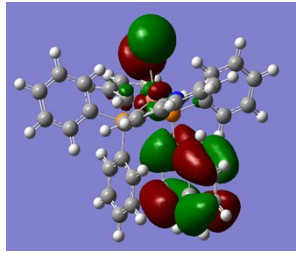
LUMO+1



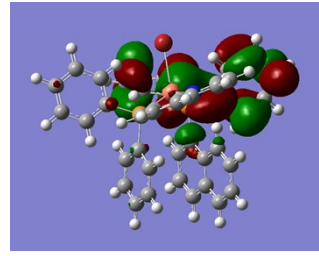
HOMO-2



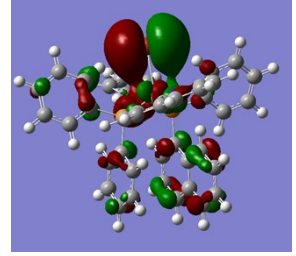
LUMO+2



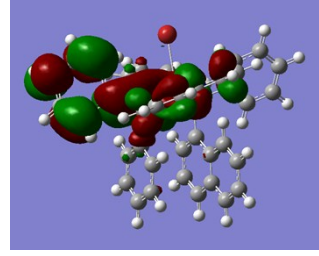
HOMO-3



LUMO+3



HOMO-4



LUMO+4

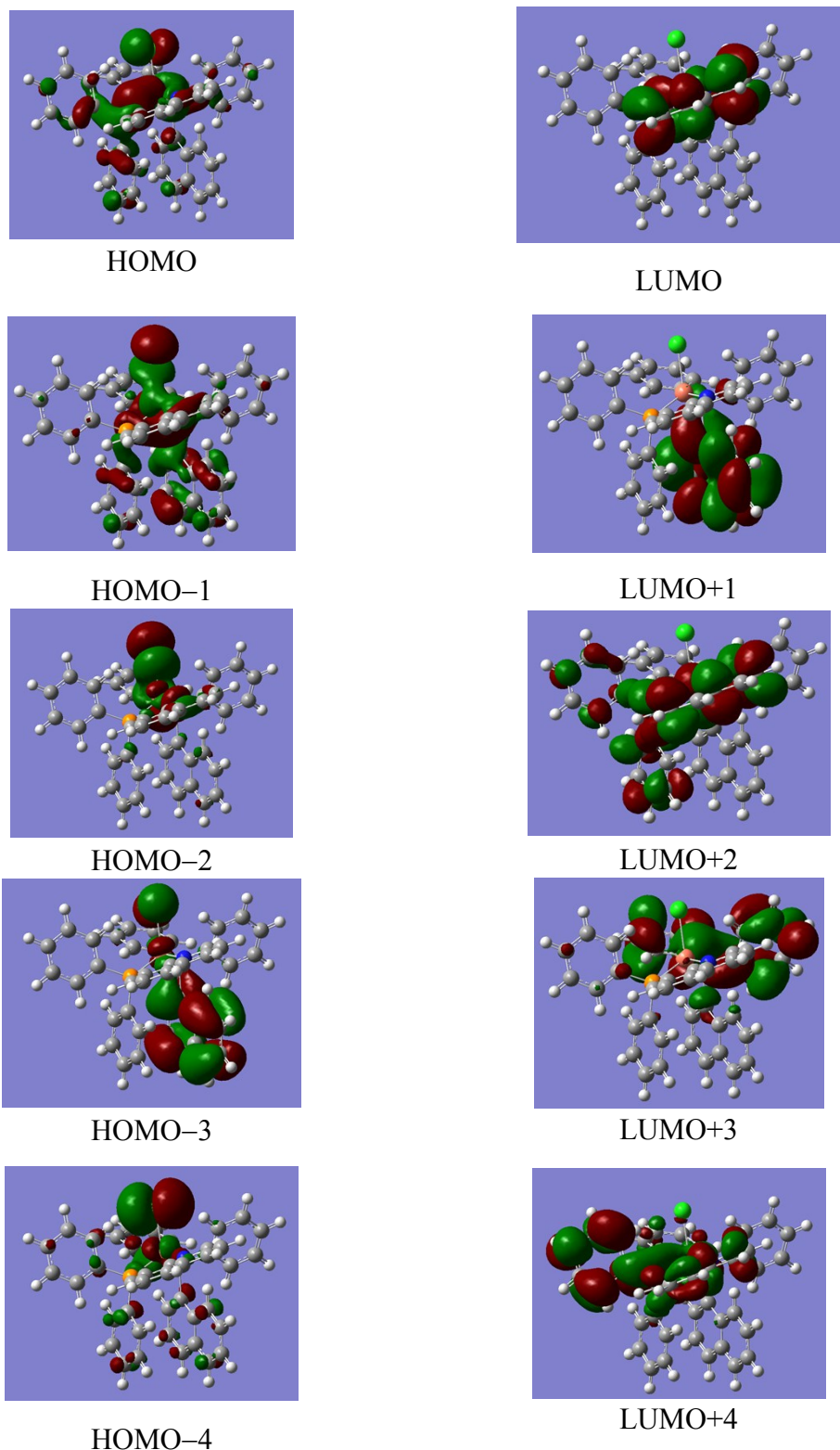


Fig. S18. Contour plots of frontier molecular orbitals of complexes **1-3** in CH_2Cl_2 .

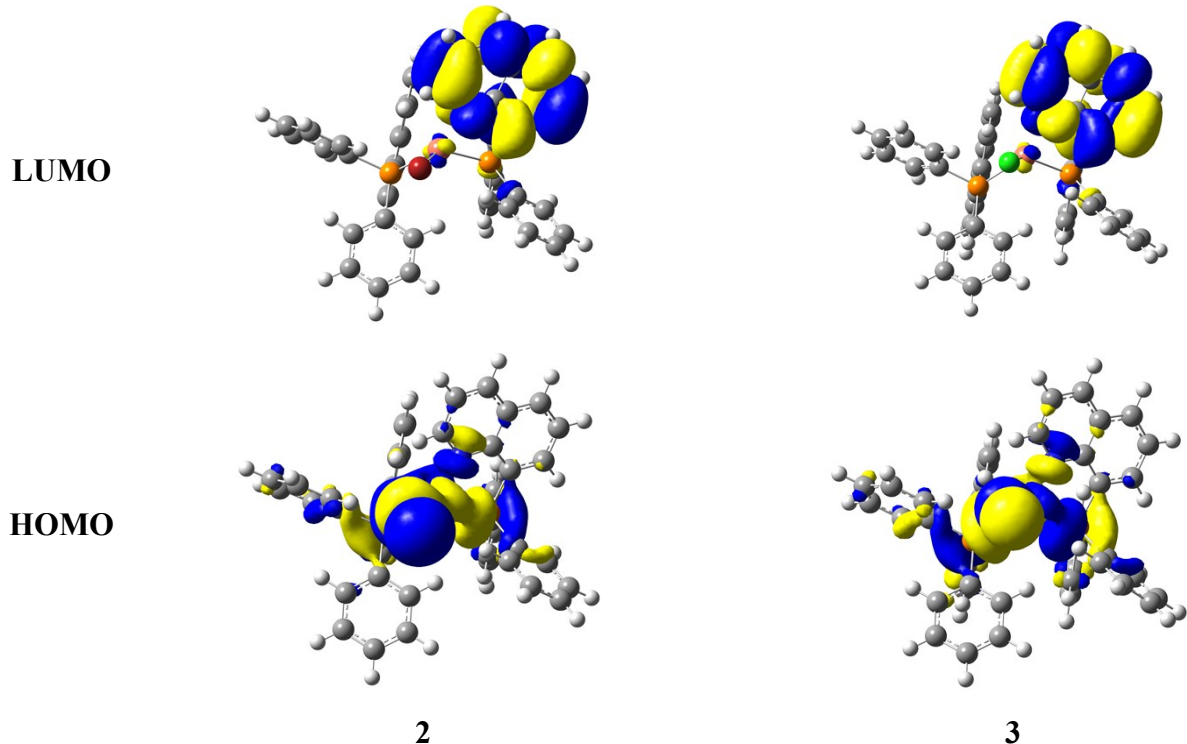


Fig. S19. Contour plots of frontier molecular orbitals at the first excited state geometries of complexes **2** and **3**

Table S1. Energy and compositions of frontiers molecular orbitals of complex **1** in CH_2Cl_2 .

MO	Energy(ev)	Cu	I	P	Quinoline ring	Naphthalene ring	Benzene ring
H-4	-6.30	18.63	54.72	4.30	5.48	5.72	11.16
H-3	-6.26	5.28	32.65	1.27	0.89	51.09	8.81
H-2	-5.95	23.57	62.13	2.71	4.39	4.13	3.07
H-1	-5.78	24.41	50.37	8.20	5.96	5.44	5.62
H ^a	-5.43	24.97	30.94	21.78	4.73	3.78	13.80
L ^b	-2.26	0.44	0.15	0.96	93.43	0.54	4.48
L+1	-1.54	0.54	0.16	1.78	2.39	85.89	9.25
L+2	-1.16	1.13	0.35	2.50	78.57	2.88	14.56
L+3	-1.07	0.81	0.28	7.35	32.40	0.65	58.50
L+4	-0.94	1.36	0.75	7.03	1.00	13.81	76.04

^a H denotes HOMO,

^b L denotes LUMO.

Table S2. Energy and compositions of frontiers molecular orbitals of complex **2** in CH₂Cl₂.

MO	Energy(ev)	Cu	Br	P	Quinoline ring	Naphthalene ring	Benzene ring
H-4	-6.48	21.42	55.94	2.14	4.01	4.86	11.64
H-3	-6.31	9.81	20.85	0.60	0.60	62.38	5.75
H-2	-6.00	39.14	43.28	3.03	7.40	3.30	3.86
H-1	-5.85	35.94	23.65	12.46	8.58	9.65	9.71
H ^a	-5.46	31.12	18.03	24.43	6.11	3.68	16.63
L ^b	-2.17	0.38	0.14	0.80	93.64	0.77	4.27
L+1	-1.47	0.61	0.13	1.51	1.53	85.89	10.32
L+2	-1.07	0.30	0.13	1.50	77.40	2.09	18.58
L+3	-0.95	0.55	0.24	5.54	5.09	32.37	56.22
L+4	-0.91	1.13	0.38	7.72	33.89	1.74	55.15

^a H denotes HOMO,^b L denotes LUMO.**Table S3.** Energy and compositions of frontiers molecular orbitals of complex **3** in CH₂Cl₂.

MO	Energy(ev)	Cu	Cl	P	Quinoline ring	Naphthalene ring	Benzene ring
H-4	-6.63	38.80	40.29	1.62	2.95	2.93	13.41
H-3	-6.29	12.28	9.39	1.51	0.43	69.93	6.46
H-2	-6.06	51.46	29.03	3.76	7.63	3.68	4.43
H-1	-5.84	41.59	12.60	13.05	9.80	12.25	10.71
H ^a	-5.42	34.25	11.37	25.99	6.54	4.10	17.75
L ^b	-2.16	0.39	0.12	0.78	93.56	0.85	4.30
L+1	-1.53	0.58	0.09	1.38	1.56	87.28	9.11
L+2	-1.06	0.48	0.14	2.59	64.03	3.99	28.77
L+3	-0.98	0.32	0.10	5.33	8.70	22.45	63.10
L+4	-0.93	1.15	0.39	6.98	35.79	1.31	54.38

^a H denotes HOMO,^b L denotes LUMO.

Table S4. Computed excitation states for complex **1** in CH₂Cl₂.

State	$\lambda(\text{nm})/E(\text{eV})$	Configurations	f
1	461.8 (2.68)	H-1→L (4); H→L(92)	0.0013
2	429.4 (2.89)	H-1→L (6); H→L (92)	0.0087
3	412.4 (3.01)	H-2→L(94)	0.0073
4	375.6 (3.3)	H-3→L (92)	0.0007
5	360.5 (3.44)	H→L+1 (98)	0.0283
7	346.5 (3.58)	H-1→L+1 (96)	0.0457
9	328.1 (3.78)	H-2→L+1 (4); H-1→L+2 (4); H→L+2 (86)	0.0176
11	318.6 (3.89)	H-1→L+3 (4); H→L+3 (92)	0.0187
12	313.9 (3.95)	H-1→L+4 (4); H→L+4(78); H→L+5(8)	0.0340
13	312.4 (3.97)	H-1→L+2 (90); H→L+2 (6)	0.0110
14	307.7 (4.03)	H-1→L+3 (26); H→L+4 (8); H→L+5 (50); H→L+6 (4)	0.0717
15	306.2 (4.05)	H-6→L (58); H-4→L+1 (4); H-3→L+1 (28)	0.0893
16	305.2 (4.06)	H-1→L+3 (62); H→ L+3 (4); H →L+5 (18)	0.0118
17	304.9 (4.07)	H-6→ L (24); H-3→ L+1 (58); H-1→ L+3 (4); H → L+7 (6)	0.0360
19	302.6 (4.10)	H-6→ L (4); H-2→ L+2 (4); H →L+7 (82)	0.0550
20	300.2 (4.13)	H-4→ L+1 (76); H-3→ L+1 (6); H →L+6 (6)	0.0472
21	299.1 (4.15)	H-4→ L+1 (10); H → L+5 (6); H → L+6 (66)	0.0135
22	297.3 (4.17)	H-2→ L+3 (4); H-1→ L+4 (64); H-1→ L+5 (10); H → L+4 (6)	0.0312
24	293.5 (4.22)	H-2→ L+3 (18); H-1→ L+4 (6); H-1→ L+5 (56); H → L+6 (8)	0.0224
29	288.5 (4.29)	H-2→ L+4 (68); H-2→ L+5 (6); H-1→ L+6 (10)	0.0482
32	285.8 (4.34)	H-5→L+1 (86); H-1→ L+6 (4)	0.0213
33	284.7 (4.35)	H-16→ L (6); H-14→ L (22); H-10→ L (6); H-9→ L (16); H-8→ L (28)	0.0121
39	280.1 (4.43)	H-18→ L (6); H-16→ L (10); H-1→ L (16); H-9→ L (8); H-2→ L+5 (22); H-2→ L+7 (8)	0.0590

Table S5. Computed excitation states for complex **2** in CH₂Cl₂.

State	$\lambda(\text{nm})/E(\text{eV})$	Configurations	f
1	464.6 (2.67)	H-1→L (4); H→L(94)	0.0013
2	420.5 (2.95)	H-1→L (94); H→L (4)	0.0081
3	397.1 (3.12)	H-2→L (96)	0.0081
4	363.3 (3.41)	H→L+1 (98)	0.0254
6	348.8 (3.61)	H-4→L (46); H-3→L (24); H-1→L+1 (26)	0.0126
7	343.6 (3.61)	H-3→L (6); H-1→L+1 (72)	0.0344
8	329.7 (3.76)	H-1→L+2 (4); H→L+2 (92)	0.0183
11	318.5 (3.89)	H→L+3 (90); H→L+4 (4)	0.0195
12	316.7 (3.91)	H-1→L+4 (4); H→L+3 (6); H→L+4 (78); H→L+5 (6)	0.0351
13	308.6 (4.02)	H-1→L+2 (20); H-1→L+3 (4); H→L+4 (6); H→L+5 (56), H→L+6 (6)	0.0373
14	307.7 (4.03)	H-1→L+2 (70); H→L+5 (16)	0.0362
15	305.4 (4.06)	H-6→L (82); H→L+7 (6)	0.1166
16	303.0 (4.09)	H-6→L (6); H→L+6 (12); H→L+7 (72)	0.0686
17	301.6 (4.11)	H-3→L+1 (4); H-1→L+3 (84); H→L+3 (4); H→L+5 (4)	0.0225

18	300.0 (4.13)	H-7→L+1 (4); H-3→L+1 (6); H-1→L+6 (4); H→L+5 (8); H→L+6 (60); H→L+7 (12)	0.0123
19	197.4 (4.17)	H-3→L+1 (80); H-1→L+3 (4); H→L+6 (6)	0.0601
21	294.5 (4.21)	H-1→L (6); H-10→L (22); H-8→L (4); H-2→L+2 (36); H-1→L+4 (14)	0.0132
22	293.5 (4.22)	H-17→L (4); H-10→L (28); H-8→L (8); H-1→L+4 (38); H-1→L+5 (4)	0.0251
23	290.5 (4.27)	H-7→L+1 (4); H-1→L+4 (10); H-1→L+5 (70); H→L+6 (6)	0.0191
25	288.7 (4.29)	H-7→L (10); H-7→L+1 (8); H-4→L+1 (30); H-1→L+6 (34); H-15→L (4); H-14 (14); H-11→L (12); H-10→L (12); H-9→L (8); H-8→L (20); H-2→L+3 (16)	0.0141
31	283.6 (4.37)	H-14→L (4); H-12→L (4); H-9→L (6); H-2→L+4 (60); H-2→L+5 (8); H-1→L+5 (4)	0.0149
32	282.4 (4.39)	H-18→L (8); H-16→L (6); H-12→L (8); H-11→L (8); H-9→L (12); H-8→L (6); H-6→L+2 (6); H-2→L+4 (12); H-2→L+5 (6)	0.0310
33	282.2 (4.39)	H-18→L (4); H-16→L (8); H-13→L (4); H-12→L (18); H-9→L (6); H-6→L+2 (4); H-5→L+1 (22); H-1→L+5 (4); H→L+10 (12)	0.0131
34	280.0 (4.43)		0.0373

Table S6. Computed excitation states for complex **3** in CH₂Cl₂.

State	$\lambda(\text{nm})/E(\text{eV})$	Configurations	f
1	467.0 (2.66)	H→L (96)	0.0011
2	418.4 (2.96)	H-1→L (94); H→L (4)	0.0067
3	390.8 (3.17)	H-2→L (96)	0.0088
4	365.8 (3.39)	H→L+1 (98)	0.0224
6	343.4 (3.61)	H-3→L (10); H-1→L+1 (86)	0.0422
8	330.7 (3.75)	H-4→L (12); H→L+2 (84)	0.0181
10	319.4 (3.89)	H-5→L (50); H→L+3 (26); H→L+4 (14)	0.0309
11	318.9 (3.89)	H-5→L (18); H→L+4 (68); H→L+5 (4)	0.0244
13	309.0 (4.01)	H-1→L+2 (4); H→L+4 (6); H→L+5 (64); H→L+6 (16)	0.0471
14	306.7 (4.04)	H-1→L+2 (84); H→L+7 (4)	0.0249
15	304.2 (4.07)	H-6→L (30); H→L+6 (8); H→L+7 (54)	0.0977
16	302.9 (4.09)	H-6→L (60); H-1→L+3 (4); H→L+6 (6); H→L+7 (20)	0.1000
17	301.1 (4.11)	H-1→L+3 (78); H→L+5 (6); H→L+6 (6)	0.0162
18	300.9 (4.12)	H-7→L+1 (4); H-1→L+3 (6); H→L+5 (12); H→L+6 (50); H→L+7 (16)	0.0117
19	295.5 (4.19)	H-3→L+1 (82); H-1→L+4 (4); H-1→L+5 (4)	0.0702
20	294.2 (4.21)	H-3→L+1 (4); H-2→L+2 (4); H-1→L+4 (56); H-1→L+7 (6); H→L+4 (4); H→L+8 (8)	0.0327
24	289.7 (4.28)	H-7→L+1 (8); H-1→L+4 (4); H-1→L+5 (56); H→L+6 (6)	0.0207
28	284.6 (4.37)	H-13→L (6); H-11→L (6); H-10→L (18); H-8→L (46); H-2→L+2 (4); H-1→L+7 (4)	0.0134
31	280.7 (4.42)	H-13→L (4); H-4→L+1 (36); H-2→L+4 (22); H-2→L+5 (12)	0.0609

Table S7. Calculated emission wavelength (λ), oscillator strength (f) and main configuration of complexes **2-3** along with their experimental values (λ_{exp}).

	λ (nm)	f	Main configurations	λ_{exp} (nm)
2	672	0.005	HOMO→LUMO (95%)	685
3	695	0.004	HOMO→LUMO (96%)	691